Technical University of Denmark

DTU

Transitions between beta and gamma rhythms in neural systems

Sosnovtseva, Olga; Setsinsky, D.; Fausbøll, Anders; Mosekilde, Erik

DTU Library
Technical Information Center of Denmark

Transitions between β and γ rhythms in neural systems

O. V. Sosnovtseva,[1] D. Setsinsky,[1] A. Fausbøll,[2] and E. Mosekilde[2]
[1]*Physics Department, Saratov State University, Astrahanskaya Street 83, Saratov 410026, Russia*
[2]*Department of Physics, The Technical University of Denmark, 2800 Kongens. Lyngby, Denmark*
(Received 29 April 2002; published 9 October 2002)

We study the coexistence of different rhythms in a local network of one inhibitory and two excitatory nerve cells for a wide range of the excitatory synapse strength and of the slow K^+-channel conductance. The dynamic features of spike trains in the presence of noise are discussed. It is found that noise can both cause switching between different states and induce coherent firing events.

I. INTRODUCTION

The spatiotemporal characteristics of neural firing patterns in connection with brain function have received considerable interest, and many studies have been performed in order to understand the origin and role, as well as the dynamics of synchronized neural activity (e.g., Ref. [1,2]). Many neural systems can perform oscillations in different modes. The thalamocotical relay neurons, for instance, can generate either spindle or δ oscillations [3]. Recently, Neiman and Russell [4] have found that the electroreceptors in paddlefish possess the property of being biperiodic. Moreover, brain oscillations are normally divided into different types based mainly on their frequency. Rhythms in the β (12–30 Hz) and the γ (30–80 Hz) ranges are found in many parts of the nervous system and are associated with attention, perception, and cognition [5–7]. The same rhythms appear in the neocortex as well as in the hippocampus. It has been shown that a model of inhibitory, gamma-aminobutyric acidergic (GABA) interneurons of the hippocampus can generate γ rhythms [8]. Recently, Kopell *et al.* [9] demonstrated that a model including both inhibitory interneurons and excitatory pyramidal cells can produce β as well as γ oscillations. It has been noted in electroencephalogram signals that rhythms of different frequencies can be found simultaneously [10]. The experimental and modeling studies have suggested that rhythms in the hippocampus employ different dynamical mechanisms to synchronize [11,12]. The β mode is able to synchronize with long conduction delays corresponding to signals traveling over a significant distance in the brain. Similar distances cannot be tolerated by the γ rhythms that are used for more local communications.

In most cases the effects of noise on neural firing have not been considered. Neural activity is known to be noisy [13], and this stochastic feature is observed during both information transmission and spontaneous firing. At the same time, noise can play a constructive role in neural systems. In the presence of a subthreshold signal, the excitation threshold may be crossed whenever the signal has a maximum, as the noise is superimposed onto the signal. This mechanism allows the biological system to detect signals that nearly disappear in the noise background [14,15], demonstrating the effect of stochastic resonance [16]. Without periodic forcing an excitable neuronal system can exhibit the related phenomenon of coherence resonance [17–19]. Stochastic synchroni-

zation phenomena in electrosensitive cells of the paddlefish have been studied in electrophysiological experiments by Neiman *et al.* [20]. Different types of noisy phase locked regimes were observed. Hence, the interesting question arises: How is the dynamics of neural firing with *multimode* behavior affected by noise?

II. MODEL

We consider a minimal model for a neural network capable of producing both β and γ oscillations developed by Kopell *et al.* [9]. The model includes two excitatory pyramidal neurons and one inhibitory interneuron as shown in Fig. 1.

The Kopell model is based on Hodgkin-Huxley-type neurons [21]. The voltage of an excitatory neuron is controlled by the following differential equation:

$$c\dot{V} = -g_l(V - E_l) - g_{Na}m^3h(V - E_{Na}) - g_Kn^4(V - E_K)$$
$$- g_{ahp}w(V - E_K) - i^e_{syn} + i^e_{appl}. \qquad (1)$$

One recognizes the leak current $g_l(V - E_l)$, the sodium current $g_{Na}m^3h(V - E_{Na})$, the potassium current $g_Kn^4(V - E_K)$, and the applied current i^e_{appl}. In addition, another type of potassium current is present. This is a slow K current, creating an *after-hyperpolarization* (AHP) following a spike
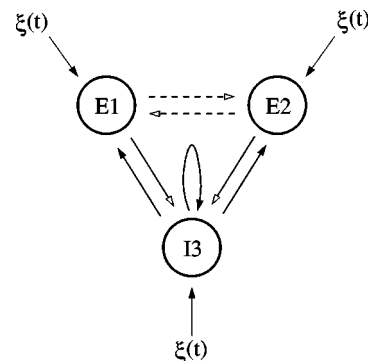

FIG. 1. Architecture of the Kopell oscillatory network. $E1$ and $E2$ are excitatory cells, $I3$ is an inhibitory cell. Open and filled arrowheads indicate excitatory and inhibitory connections, respectively. Solid lines indicate fixed connections and the dash-dotted lines represent synapses whose efficacies are varied in the simulations.

in one of the excitatory neurons. V is the membrane potential, E_j, j = Na, K, is the Nernst (or reversal) potentials for the respective ions, and g_j is the corresponding conductances. c is the membrane capacitance.

The gating variables obey the following dynamical equations:

$$\dot{m} = \alpha_m(V)(1-m) - \beta_m(V)m, \tag{2}$$

$$\dot{h} = \alpha_h(V)(1-h) - \beta_h(V)h, \tag{3}$$

$$\dot{n} = \alpha_n(V)(1-n) - \beta_n(V)n, \tag{4}$$

$$\dot{w} = \alpha_w(V)(1-w) - \beta_w(V)w, \tag{5}$$

where the α and β functions describe the voltage-dependent opening and closing rates of a particular channel, respectively. For each excitatory neuron, a single equation controls the state of the synapses going from this neuron to others:

$$\dot{s}_e = \alpha_{s_e}(V)(1-s_e) - \beta_{s_e}s_e. \tag{6}$$

Synaptic input to an excitatory neuron (here, $E1$) results in a current

$$i^e_{syn,E1} = g_{ee}s_{e,E2}(V-E_e) + g_{ie}s_{i,I3}(V-E_i). \tag{7}$$

Notice that the s variables refer to the presynaptic neurons ($E2$ and $I3$, respectively), whereas the V refers to the postsynaptic neuron (here, $E1$). E_e and E_i denote the reversal potentials associated with excitatory and inhibitory synapses, respectively. A similar equation is used for the synaptic current of $E2$.

The inhibitory neuron $I3$ is very similar to $E1$ and $E2$, only the AHP current is not included:

$$c\dot{V} = -g_l(V-E_l) - g_{Na}m^3h(V-E_{Na}) - g_Kn^4(V-E_K)$$
$$- i^i_{syn} + i^e_{appl}. \tag{8}$$

Noting that there is no need for w, the remaining gating variables for $I3$ are controlled by Eqs. (2)–(4).

Inhibitory synapses are governed by the equation

$$\dot{s}_i = \alpha_{s_i}(V)(1-s_i) - \beta_{s_i}s_i. \tag{9}$$

The inhibitory neuron receives inputs from $E1$ and $E2$ as well as from a mechanism of self-inhibition:

$$i^i_{syn,I3} = (g_{ei}s_{e,E1} + g_{ei}s_{e,E2})(V-E_e) + g_{ii}s_{i,I3}(V-E_i). \tag{10}$$

The detailed description of the various functions and parameter values can be found in the original paper [9]. Two parameters are varied in the present study: g_{ee}, the strength of
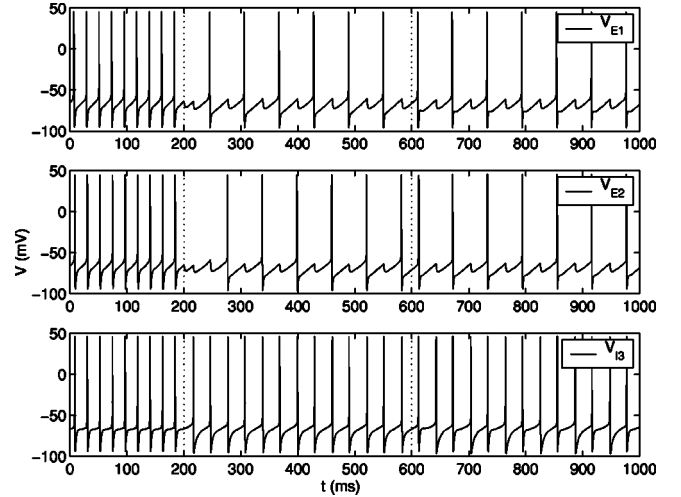

FIG. 2. From top to bottom, the voltages of $E1$, $E2$, and $I3$, respectively. For $t<200$ ms, $g_{ee}=g_{ahp}=0.0$ mS/cm^2 producing a γ rhythm of about 45–50 Hz. At $t=200$ ms, a slowly varying potassium current is added by setting $g_{ahp}=1.25$ mS/cm^2. This makes $E1$ and $E2$ switch to β rhythms of 16–17 Hz. Since the spikes of $E1$ and $E2$ are out of phase, the population of excitatory neurons considered as a whole still produces oscillations in the γ band. Finally, at $t=600$ ms, the E-E connections are added by setting $g_{ee}=0.15$ mS/cm^2. This synchronizes $E1$ and $E2$, producing a β rhythm in the the E population. For this plot, a transient of 100 ms was removed. In the notation of the present paper, the modes depicted here will be called γ, γ_{pop}, and β, going from left to right.

the connections between $E1$ and $E2$; and g_{ahp}, the maximal conductance for the slow potassium ion channels.

The above model demonstrates three main network modes (Fig. 2):

(i) For low values of the two parameters, the three neurons spike in synchrony with a frequency in the γ band.

(ii) If g_{ahp} is increased, the $E1$ and $E2$ neurons miss every other spike, lowering their individual frequencies into the β band. But since $E1$ and $E2$ are out of phase, the population of excitatory neurons as a whole continues to produce γ oscillations.

(iii) Increasing the connection strengths between $E1$ and $E2$ makes the excitatory neurons spike simultaneously, thereby producing β oscillations.

III. DETERMINISTIC DYNAMICS

A scan over a two-dimensional parameter space was carried out for g_{ahp} varied in the range [0.00 mS/cm^2 through 2.00 mS/cm^2] and g_{ee} varied in the range [0.00 mS/cm^2 through 0.30 mS/cm^2]. The initial conditions were identical for all calculations.

To determine the spiking mode, the regular spiking of $I3$ is used. First, the temporal location of the $I3$ spikes is determined. Thereupon, a window of ± 5 ms around the $I3$ spikes is searched for possible spikes in $E1$ and $E2$. For each point in the diagram, spike trains for $E1$ and $E2$ are thereby produced. Hence, the oscillation mode is characterized by these spike trains. A restriction is put upon this automated deter-
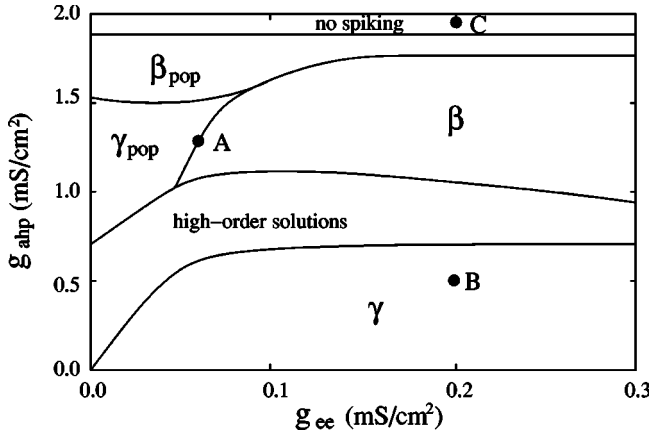
FIG. 3. Different oscillation modes as functions of g_{ee} (the coupling between excitatory neurons) and g_{ahp} (the conductance for the slow K channel in excitatory neurons).

mination procedure, namely that the period of the oscillation mode must be less that half the length of the spike trains, thereby ensuring at least two occurrences of the full period.

The results are depicted in Fig. 3. Here, one can distinguish four to five different oscillatory modes. The first state γ corresponds to γ rhythms when all neurons ($E1$, $E2$, $I3$) spike in every cycle. The "γ population" state γ_{pop} is located to the left with intermediate values of g_{ahp}. In this case, neurons $E1$ and $E2$ demonstrate β rhythms of 16–17 Hz, but their overall behavior is seen to produce oscillations in the γ band. There is a large region β occupied by β oscillations where $E1$ and $E2$ are in full synchrony with half the frequency of the γ rhythm. With descreasing g_{ahp}, they evolve into the β population β_{pop}. This state produces a β rhythm, but only half as powerful as the β state described earlier since only one excitatory neuron $E1$ spikes. Within a range of parameters, one can observe high-order solutions with different combinations of spiking and silent states in the two excitatory neurons. The dynamics seem to be limited in the g_{ahp} direction by the appearance of a silent state, in which $E1$ and $E2$ never spike due to the effects of the AHP current in combination with the spontaneous spiking of the $I3$ neuron.

If instead of using a simulation for each diagram point, we just let a simulation run while gradually changing the g_{ee} parameter, the border at $g_{ee} \approx 0.043\,08$ mS/cm^2 disappears. A forward-and-backward adiabatic scan reveals that the γ_{pop} mode and the β mode coexist for $g_{ee} \in [0.0286$ mS/cm^2; 0.0768 mS/cm$^2]$ (Fig. 4). The observa-
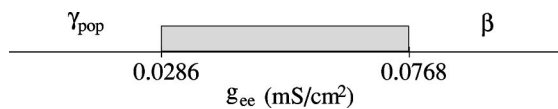

FIG. 4. One-parameter scan for $g_{ahp} = 1.25$ mS/cm^2. The scan starts in the γ_{pop} mode in the left end of the axis, switching to the β mode when the γ_{pop} mode becomes unstable at $g_{ee} = 0.0768$ mS/cm^2. The reverse scan, started to the right in the β mode, switches to the γ_{pop} mode only when $g_{ee} = 0.0286$ mS/cm^2 is reached. In the gray region, the two modes coexist.
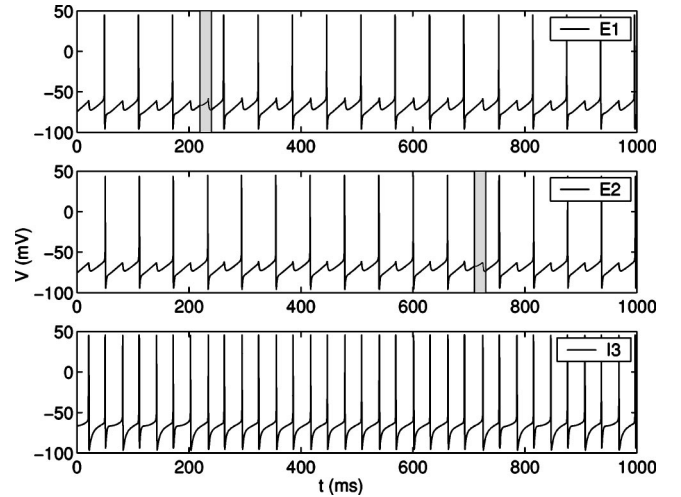

FIG. 5. A simulation for $g_{ee} = 0.05$ mS/cm^2 and $g_{ahp} = 1.25$ mS/cm^2. For these parameter values, the γ_{pop} and β solutions coexist. The system starts out in the synchronous β mode. For $t \in [220$ ms; 240 ms] (marked with the upper, gray box), the applied current to the $E1$ neuron $i_{appl,E1}$ is temporarily lowered from 5.5 μA/cm^2 to 4.5 μA/cm^2. This makes the $E1$ neuron miss a spike, changing the overall spiking mode to the asynchronous γ_{pop} mode. Conversely, when for $t \in [710$ ms; 730 ms] (marked with the lower, gray box), the value of $i_{appl,E2}$ is lowered from 5.0 μA/cm^2 to 4.0 μA/cm^2, the spiking mode changes back to β.

tion of a large region with coexisting solutions may have important interpretations with respect to the brain function.

One question is: Can the Kopell model switch between the coexisting states? Since the γ_{pop} and β modes are both stable, the model does not switch spontaneously. One must somehow poke it externally to make it change to another dynamical state. In Fig. 5, this has been done by temporarily applying an additional external current of 1 μA/cm^2 to either $E1$ or $E2$. This can cause one of the neurons to miss a spike, thereby changing the spiking mode back and forth between the coexisting γ_{pop} and β modes. Physiologically, this extra applied current, together with ionic and synaptic currents, could represent the influence of other neurons of the brain. This influence may in many instances be considered as stochastic. Let us, therefore, consider the influence of fluctuations on the switching process.

IV. STOCHASTIC DYNAMICS

Since noise may have different origins and can contribute in different ways, we assume that our network operate in a noisy field (Fig. 1). We model it as Gaussian noise $\xi(t)$ with intensity D added to the first equations of each neuron.

Transition between coexisting γ_{pop} and β. With noise of sufficient intensity, the system switches between two states. This can be characterized in different ways. First, we can introduce a shift between the spiking events in $E1$ and $E2$ as $\Delta\phi = 2\pi t/T$. In this case, the system can be considered as bistable where a trajectory alternates between $\Delta\phi = 0$ and $\Delta\phi = \pi$ [Fig. 6(a)]. With increasing noise intensity, hopping becomes more frequent. Second, the system can be described via the overall dynamics of the excitatory neurons. Let us
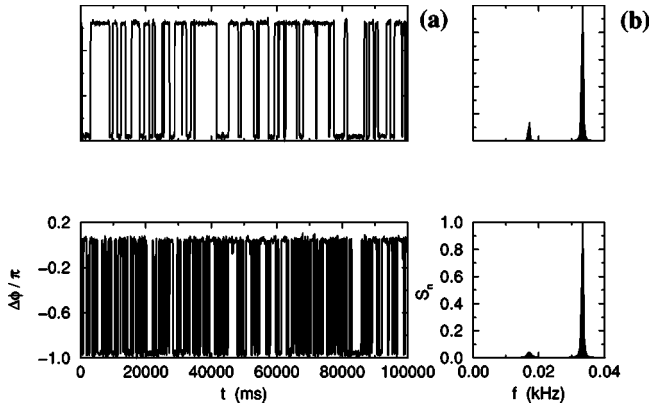
FIG. 6. (a) Switching processes between two modes and (b) normalized power spectra for the output signals from the excitatory neurons. The noise intensity is increased from top to bottom: $D = 0.15$ and 0.24, respectively ($g_{ahp} = 1.25$ mS/cm^2, $g_{ee} = 0.05$ mS/cm^2).

choose the parameters to be in the region where γ_{pop} and β oscillations coexist (point A in Fig. 3). In the noiseless case, with the applied initial conditions, the resulting output oscillations is of β rhythm. This corresponds to a sharp peak at $f_\beta = 17$ Hz. With noise, an additional peak appears at $f_\gamma = 34$ Hz [Fig. 6(b)]. With increasing noise, the peak at f_β becomes broader and smaller in amplitude.

To describe the switching dynamics, we can calculate different characteristics. Figure 7(a) illustrates the behavior of the residence time (solid and dotted curves) in the bistable system with $\Delta\phi = 0$ and $\Delta\phi = \pi$. With vanishing noise, the system is in the $\Delta\phi = 0$ state, i.e., the residence time tends to infinity. When noise is introduced, the system switches to
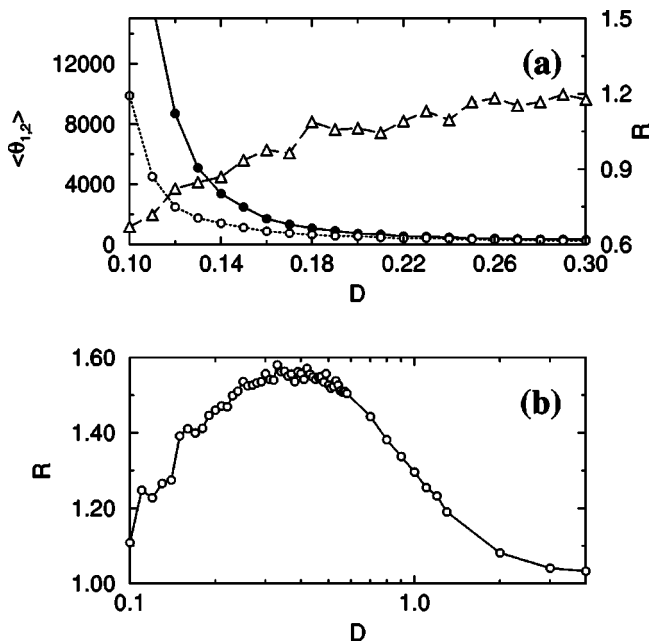

FIG. 7. (a) Residence time for $\Delta = 0$ (solid curve) and $\Delta = \pi$ (dotted curve) and coherence of switching time (dashed curve) as functions of the noise amplitude; (b) regularity calculated over interspike intervals ($g_{ahp} = 1.25$ mS/cm^2, $g_{ee} = 0.05$ mS/cm^2).

another state. With increasing noise, the residence times in the two states become equal.

A quantitative measure of coherence is the so-called regularity coefficient that can be calculated as [19]

$$R = \langle \tau \rangle / \sqrt{\langle \tau^2 \rangle - \langle \tau \rangle^2}, \qquad (11)$$

where τ is specified as the switching time between the states [Fig. 7(a), dashed curve] or as the interspike interval [Fig. 7(b)]. The time averaged duration identifies the mean period and, hence, the mean frequency $\langle f \rangle = 1/\langle \tau \rangle$ of the noise-activated oscillations. Figure 7(a) illustrates how the coherence of the switching events (dashed curve) grows monotonically when the noise intensity is increased. Very strong noise causes fast switching. The residence time then becomes less than 2 interspike periods, and our two-state approach no longer works.

The spike train provides an efficient way to code a sequence of action potentials with nearly the same shape since the most important information in neuronal systems is widely believed to be coded in the time sequence of action potential generation [22]. The spike train is a binary time series with a value of 1 at the time of action potential generations and 0 at other times. We analyzed the coherence properties for spike trains in the presence of noise. The results of a calculation of regularity (11) as a function of noise intensity are shown in Fig. 7(b). It is seen to display a maximum. For weak noise, the contribution of γ_{pop} to the whole spike train is small. For optimal noise intensity, β and γ_{pop} contribute equally to a spiking train. Strong noise destroys the β rhythm, and the regularity decreases. This represents an example of coherence resonance in the noise-induced switching between the different modes of the neural system.

Transition between γ and β. In diagram presented in Fig. 3, regions of γ and β rhythms are separated by the region of high-periodic solutions. Fixing the parameters at the point B (Fig. 3), with noise added, we observe a *direct* transition between the main rhythms (Fig. 8). It is clearly seen how the residence time in the β regime grows with increasing noise intensity. The measure of coherence calculated over interspike intervals indicates a well-pronounced maximum at some optimal noise intensity at which β and γ spike trains alternate in a regular way (Fig. 9). Here, we observe another example of regularized hopping events induced by applied noise but now with one of the involved states being unstable for the considered parameters.

Transition to spiking dynamics. Let us hereafter see how noise can cause firing events in this local network. (Parameters are at point C in Fig. 3). It is known that the behavior of spike trains can exhibit coherence resonance at optimal noise intensity as described for a single Hodgkin-Huxley model [18]. In this case, noise affects the dynamics of the system in two ways:

(i) The increase of noise intensity decreases the silence (activation) time so that the contribution of the spiking dynamics increases (Fig. 9). This tendency enhances the regularization of spiking dynamics of the membrane potential.
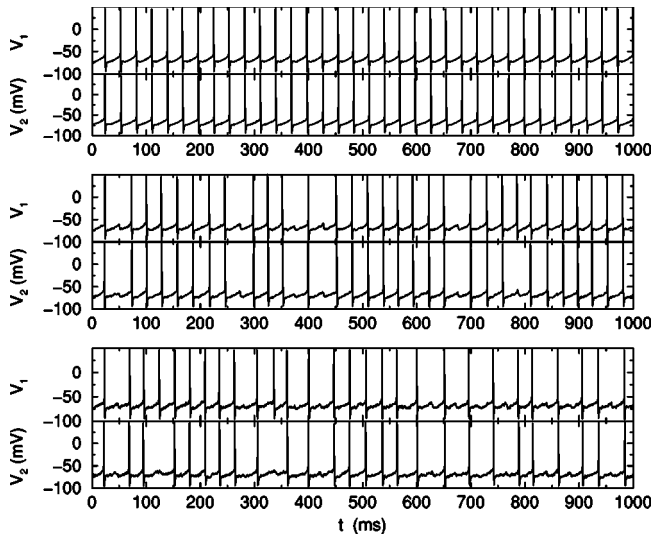
FIG. 8. Switching process between γ and β rhythms for g_{ahp} = 0.5 mS/cm^2 and g_{ee} = 0.2 mS/cm^2. With increasing noise amplitude: D = 0.2 (top trace), 0.8 (middle trace), and 1.5 (bottom trace).

(ii) Noise also results in the amplitude and in phase fluctuations of the firing dynamics destroying the periodicity in spiking events.

The competition of these two mechanisms produces the coherence resonance, i.e., a maximal coherence for an optimal noise level. This mechanism is responsible for the first peak of coherence for $E1$ (Fig. 10). With vanishing connection between excitatory cells (g_{ee} = 0 mS/cm^2), $E2$ demonstrates coherence of spiking events at higher noise intensity because of different internal parameters. Remarkably, due to inhibitory synapses (controlled directly in the Kopell model by varying the g_{ii} and g_{ie}), the first neuron adjusts its spiking train and demonstrate secondary coherence resonance at higher noise intensity [Fig. 10(a)]. When the $E1$-$E2$ connection is introduced (g_{ee} = 0.2 mS/cm^2), the two peaks ap-
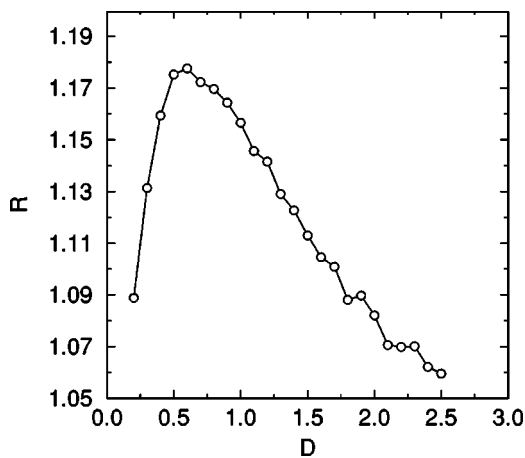

FIG. 9. Coherence dynamics of interspike intervals for g_{ahp} = 0.5 mS/cm^2 and g_{ee} = 0.2 mS/cm^2.
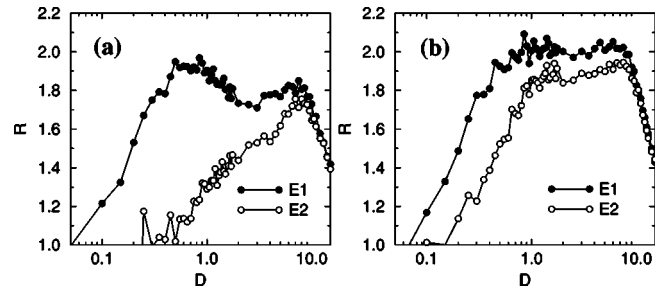

FIG. 10. Regularity for (a) g_{ahp} = 2.0 mS/cm^2, g_{ee} = 0.0 mS/cm^2 and (b) g_{ahp} = 2.0 mS/cm^2, g_{ee} = 0.2 mS/cm^2. Note how the two peaks observed in (a) are closer to one another in (b).

proach one another [Fig. 10(b)]. The excitable units demonstrate a well-pronounced peak of coherence at the same noise intensity. The maximal value of R is higher than in the previous case because of synchronization effects [23].

V. DISCUSSION

We demonstrated a series of synchronization transitions in a system of three coupled neural cells generating β and γ rhythms. For the deterministic model, the overall activity is controlled by the conductance of a slow K$^+$ channel and by the connection strength between the excitatory neurons. Eighteen different spiking modes have been identified [24]. Within a wide range of parameters two main oscillatory modes, referred to as β and γ rhythms, coexist. It was shown how the system can change back and forth between these two regimes if a small additional input current is added in short periods of time.

Next, we explored the effect of noise on the system displaying different spiking patterns. In the area with coexisting solutions, noise causes the network to jump from one state to the other. The all-or-nothing effect of being either in one oscillatory mode or in hopping between them depends on the noise intensity. The output signal demonstrates quite "regular" switchings for a certain noise intensity. Moreover, noise can initiate switchings in the region where the main β and γ oscillations are separated by high-periodic solutions in the parameter space. In this case, we again indicate an optimal noise intensity at which jumping behavior becomes coherent.

A particularly interesting finding is that, due to synaptic inhibitory interaction, the excitatory cells can demonstrate double coherence resonance. With introduction of coupling between these neurons, the two peaks of regularity merge together giving rise to further gain of regularity by virtue of synchronization.

[1] R. Eckhorn, R. Bauer, W. Jordan, M. Brosch, W. Kruse, W. Munk, and H.J. Reitboeck, Biol. Cybern. **60**, 121 (1988).

[2] C.M. Gray, P. König, A.K. Engel, and W. Singer, Nature (London) **338**, 334 (1989).

[3] X.-J. Wang, Neuroscience **59**, 21 (1994).

[4] A. Neiman and D.F. Russell, Phys. Rev. Lett. **86**, 3443 (2001).

[5] S.E. Farmer, J. Physiol. (London) **509**, 3 (1998).

[6] W. Singer, Annu. Rev. Physiol. **55**, 349 (1993).

[7] R. D. Traub, J. G. R. Jefferys, and M. Whittington, *Fast Oscillations in Cortical Circuits* (MIT Press, Cambridge, MA, 1999).

[8] X.-J. Wang and G. Buzsáki, J. Neurosci. **16**, 6402 (1996).

[9] N. Kopell, G.B. Ermentrout, M.A. Whittington, and R.D. Traub, Proc. Natl. Acad. Sci. U.S.A. **97**, 1867 (2000).

[10] R. Coppola Bressler and R. Nakamura, Nature (London) **366**, 153 (1993).

[11] P.R. Roelfsema, A.K. Engel, P. König, and W. Singer, Nature (London) **385**, 157 (1997).

[12] A. von Stein, P. Rappelsberger, J. Sarnthein, and H. Petsche, Cereb. Cortex **9**, 137 (1999).

[13] H.C. Tuckwell, *Stochastic Processes in the Neurosciences* (SIAM, Philadelphia, 1989); J.G. Taylor, in *Neurodynamics*, edited by F. Faseman and H.D. Doebner (World Scientific, Singapore, 1991), pp. 129–164.

[14] H.A. Braun, H. Wissing, K. Schäfer, and M.C. Hirsch, Nature (London) **367**, 270 (1994).

[15] D.F. Russell, L.A. Wilkens, and F. Moss, Nature (London) **402**, 291 (1999).

[16] K. Nakamura, Proc. Inst. Natural Sci. **35**, 179 (2000).

[17] A. Longtin, Phys. Rev. E **55**, 868 (1997).

[18] A. Neiman, P.I. Saparin, and L. Stone, Phys. Rev. E **56**, 270 (1997); S.-G. Lee, A. Neiman, and S. Kim, *ibid.* **57**, 3292 (1998).

[19] A.S. Pikovsky and J. Kurths, Phys. Rev. Lett. **78**, 775 (1997).

[20] A. Neiman, X. Pei, D. Russell, W. Wojtenek, L. Wilkens, F. Moss, H.A. Braun, M.T. Huber, and K. Voigt, Phys. Rev. Lett. **82**, 660 (1999).

[21] A.L. Hodgkin and A.F. Huxley, J. Physiol. (London) **117**, 500 (1952).

[22] G.P. Moore, D.H. Perkel, and J.P. Segundo, Annu. Rev. Physiol. **28**, 493 (1966).

[23] D.E. Postnov, D.V. Setsinsky, and O.V. Sosnovtseva, Tech. Phys. Lett. **27**, 49 (2001).

[24] A. Fausbøll, MSc. thesis, Technical University of Denmark, 2001.